International Journal of Advances in Engineering and Management (IJAEM)
Volume 4, Issue 5 May 2022, pp: 1190-1205 www.ijaem.net ISSN: 2395-5252

Effect of Induced Magnetic Field on Mhd Free Convective Slip-Flow of Jeffery Fluid in a Vertical Microchannel

R.Pradhan[1]. G.C. Dash[2] and S.R.Mishra[3]
[1]*Department of Mathematics, U. N Autonomous college of Science and Technology. Cuttack*
[2,3]*Department of Mathematics. I.T.E.R. Siksha 'O' Anusandhan University, Bhubaneswar*

Submitted: 10-05-2022 Revised: 19-05-2022 Accepted: 22-05-2022

ABSTRACT
The steady boundary layer stagnation-point flow of viscous incompressible flow over a permeable flat plate through porous medium has been studied. The effect of thermal radiation and chemical reaction are investigated also. The resulting partial differential equations are converted into the ordinary differential equations by the suitable transformation. The velocity and temperature profiles are computed by employing the numerical computations. It is found that the present results are in an excellent agreement with an available data. Pertinent results are presented graphically and discussed quantitatively with respect to variation in flow parameters.

Keywords: Stagnation point; Porous medium; MHD flow; Runge-Kutta fourth order; shooting technique.

I. INTRODUCTION

In nature every phenomenon that occurs is nonlinear to some extent. Linearisation is a mathematical simplification restricting small variations in physical quantities and involved parameters. A lot of work has been reported using quasi linearization principle. Many fluid properties have been investigated and found to agree with experimental result when linear law comprising stress and rate of strain components is valid. However, important technological applications of the fluids which comprise highly viscous fluid, polymeric solutions macro-molecular materials and collydos etc. have nonlinear constitutive equations. Some fluids have memory effect exhibiting elastic property. Some order fluidsposses no memory and using them to describe memory phenomena may lead to disaster.

The present model of viscoelastic fluid (Jeffery fluid) is bereft of such anomalies. Moreover, in Jeffery's element viscosity is active in every deformation. It is good for fluids not for solids. In some viscoelastic model the concept of memory of fluid or the viscoelastic property is introduced through the time derivatives of the velocity gradient tensor such as Walters and Oldroyd model.

It is interesting to analyze the flow of conducting fluid and the heat transfer in the presence of magnetic field as well as induced magnetic field. Such flows are characterized by buoyancy-induced micro pump and micro heat exchanger in micro thermal system. Micro fluidic systems have characteristic lengths of order (1-100) μm. Rarefied gaseous flows are observed very often in the micro geometric configurations. Rarefaction effects are to be considered in fluids in which the molecular mean free path (order of 100nm) is comparable to the system's characteristic length. In such case, the fluid molecular structure become more significant and the continuum assumption is no longer valid. That results in non-continuum effects such as slip-flow and thermo and solutal dynamic non-equilibrium (temperature and concentration jump) at the gas-solid interface. From above, it is evident that the rarefaction effects must be taken into account while studying the flow in microchannel.

Further, the Knudsen number (Kn), defined as the ratio of the molecular mean free path (λ_1) to the characteristic length of the system, is the parameter used to classify the fluids that deviate from continuum behavior. For small values $(Kn \leq 10^{-3})$ the fluid is considered to be continuum, while for large values $(Kn \geq 10)$, the fluid is considered to be a free molecular flow. The slip-flow regime to be studied here, is near the continuum region and is classified as $10^{-3} < Kn < 10^{-1}$ (Yu Shiping et al. [1]).

International Journal of Advances in Engineering and Management (IJAEM)
Volume 4, Issue 5 May 2022, pp: 1190-1205 www.ijaem.net ISSN: 2395-5252

Flow models in the slip-flow region obey Navier-Stokes and energy equations modified by boundary conditions that contain the rarefaction effect on the velocity and temperature fields. More recently, Liu et al.[2] and Arkilic et al. [3] found that the Navier-Stokes equations, when combined with slip-flow boundary conditions, yield results for pressure drop and friction factor that are in agreement with experimental data for some microchannel flows. Shih et al. [4], Barron et al. [5, 6] and Wang [7] have investigated this problem for an isothermal wall condition.

The metallic rectangular microchannels are useful in microthermal fluid systems. Therefore, to analyzemicroscale thermal fluid systems, rectangular microchannels are the primary mode of fluid transport. This supports strong motivation for studying slip-flow heat transfer in a rectangular vertical microchannel.

Micro-electro-mechanical systems (MEMS) and nano-electrical-mechanical systems (NEMS) are highly integrated devices for integrated cooling or heating in microreactors. Recently, microchannelheatsink, microjet impingement cooling and microheat pipe find numerous applications in modern engineering and technology. Although there are number of MEMS devices find applications, the understanding of fluid flows and heat transfer processes in such devices need careful analysis. Biswas et al. [8] numerically investigated the flow and heat transfer characteristics in the developing region of an isothermal planar microchannel by using the semi-implicit method for pressure linked equations. Moreover, the flow of an electrical conducting fluid through a channel of circular pipe in the presence of transverse magnetic field provides a useful modeling for MHD generator, pumps and accelerators.

There are flow fields which arise from differences in concentration or material constitutions alone and in conjunction with temperature effect. Atmospheric flows at all scales are given appreciably by both temperature and H_2O concentration differences.Flows in the bodies of water are driven through the comparable effects upon density, temperature, concentration of dissolved materials and suspended particulate matter. Manganaro and Hanna [9] and Saville and Churchill [10, 11] may be considered as the pioneers of the modern research on the effects of mass transfer on free convection flow.

Further, Jha et al. [12] analytically studied the fully developed steady natural convection flow of conducting fluid in a vertical parallel plate microchannel in the presence of transverse magnetic field. In their further study [13], they have found exact solution of steady fully developed natural convection flow of viscous, incompressible, and electrically conducting fluid in a vertical annular microchannel.

The above studies of conducting fluid with non-conducting bounding surfaces are related to natural convective heat transfer in a vertical microchannel without considering the induced magnetic field as well as without volumetric heat source which is of frequent occurrence in the industrial/ chemical processes. As the induced magnetic field generates its own magnetic field and induced current in the fluid which modifies the original magnetic field; subsequently the magnetic field generates forces of electromagnetic origin which affect the fluid motion. Singh et al. [14] analyzed the hydromagnetic free convective flow in the presence of induced magnetic field. Moreover, Ghosh et al. [15] have studied hydromagnetic free convective flow in conjunction with induced magnetic field. Recently, Sarveshanand and Singh [16] analytically studied the magnetohydrodynamics free convective flow between vertical parallel porous plates in the presence of induced magnetic field. Chen and Wang [17] considered an unsteady fully developed natural convectionin a vertical parallel plate microchannel flow to analyze the effects of rarefaction and fluid wall interaction.

The objective of the present study is to consider the steady flow of a conducting fluid through a microchannel with velocity slip and temperature jumps. Moreover, the effect of volumetric heat source on the development of velocity and thermal boundary layers, is a matter of special interest. As regards to the solutions of the governing coupled system of linear equations, we have solved it analytically as well as numerically. It is found that the MAT LAB code developed for the Runge-Kutta method is suitable and consistent with analytical result. The results of the present study can be verified by comparing with [12]. We have not considered the connective contributions in both the velocity and thermal boundary layers as we have considered slow flow. Therefore, there is no large velocity gradient. Rightly, we have neglected the viscous dissipation term also.

II. MATHEMATICAL ANALYSIS

Now, consider the fully developed steady laminar natural convection flow of an electrical conducting, viscoelastic, incompressible fluid in an infinite vertical parallel plate microchannel of width b. Let x' and y' axes denote the vertically

International Journal of Advances in Engineering and Management (IJAEM)
Volume 4, Issue 5 May 2022, pp: 1190-1205 www.ijaem.net ISSN: 2395-5252

upward parallel to the gravitational acceleration g and normal to the vertical parallel plates respectively. The plates are heated asymmetrically. The hotter and cooler plates are at temperature T_1 and T_2 respectively. Due to temperature gradient, natural convection flow occurs in the microchannel $(T_1 > T_2)$. A uniform magnetic field strength of $\vec{B}$ is applied in the direction perpendicular to the flow direction. Let u' be the velocity of the fluid along x'-axis and $\vec{B} = [B_{x'}', B_0', 0]$ be the magnetic field vector.

The present study focuses to low-speed flow and of low Prandtl number fluid. Therefore, we have neglected the convective contributions in momentum and energy equations. Moreover, it is justified to neglect viscous dissipation term and as such the Joules dissipation term in the energy equation. The boundary conditions which describe velocity slip, induced magnetic field and temperature jumps at the fluid wall interface are as per [18-20]. Under the usual Boussinesq approximations the governing equations of the system are as follows:

$$\frac{\upsilon}{1+\lambda}\frac{d^2u'}{dy'^2} + \frac{\mu_e B_0'}{\rho}\frac{dB_{x'}'}{dy'} + g\beta\left(T' - T_0\right) = 0 \quad (1)$$

$$\frac{1}{\sigma\mu_e}\frac{d^2B_{x'}'}{dy'^2} + B_0'\frac{du'}{dy'} = 0 \quad (2)$$

$$\frac{k}{\rho C_p}\frac{d^2T'}{dy'^2} + \frac{Q_0}{\rho C_p}(T' - T_0) = 0 \quad (3)$$

The boundary conditions are

$$\left.\begin{aligned} u'(y=0) &= \frac{2-\sigma_v}{\sigma_v}\lambda\frac{du'}{dy'}\ ,\ B_{x'}' = 0\ ,\ T' = T_1 + \frac{2-\sigma_t}{\sigma_t}\frac{2\gamma}{\gamma+1}\frac{\lambda}{P_r}\frac{dT'}{dy'} \text{ at } y' = 0 \\ u'(y'=b) &= -\frac{2-\sigma_v}{\sigma_v}\lambda\frac{du'}{dy'}\ ,\ B_{x'}' = 0\ ,\ T' = T_0 - \frac{2-\sigma_t}{\sigma_t}\frac{2\gamma}{\gamma+1}\frac{\lambda}{P_r}\frac{dT'}{dy'} \text{ at } y' = b \end{aligned}\right\} \quad (4)$$

Using the non-dimensional quantities

$$\left.\begin{aligned} &y = \frac{y'}{b}, U = \frac{\upsilon u'}{g\beta b^2\left(T_1 - T_0\right)}, T = \frac{T' - T_0}{T_1 - T_0},\ P_m = \upsilon\sigma\mu_e \\ &P_r = \frac{\upsilon}{\alpha}, B = \frac{\upsilon}{g\beta b^2\left(T_1 - T_0\right)}\sqrt{\frac{\mu_e}{\rho}}B_{x'}', M = \frac{B_0 b}{\upsilon}\sqrt{\frac{\mu_e}{\rho}}, S = \frac{Q_0 b^2}{\rho c_p \upsilon} \end{aligned}\right\} \quad (5)$$

in equations (1), (2), (3), (4) and (5) we have

$$\frac{d^2U}{dy^2} + (1+\lambda)\left(M\frac{dB}{dy} + T\right) = 0 \quad (6)$$

$$\frac{d^2B}{dy^2} + MP_m\frac{dU}{dy} = 0 \quad (7)$$

$$\frac{d^2T}{dy^2} + PrS\theta = 0 \quad (8)$$

International Journal of Advances in Engineering and Management (IJAEM)
Volume 4, Issue 5 May 2022, pp: 1190-1205 www.ijaem.net ISSN: 2395-5252

$$\left.\begin{aligned} U(y=0) &= \beta_n Kn \frac{dU}{dy},\ B=0,\ T=\xi+\beta_n KnPn\frac{dT}{dy},\ \text{at } y=0 \\ U(y=b) &= -\beta_n Kn \frac{dU}{dy},\ B=0, T=1-\beta_n KnPn\frac{dT}{dy},\ \text{at } y=1 \end{aligned}\right\} \quad (9)$$

where

$$\left.\begin{aligned} Pn &= \frac{\beta_t}{\beta_n},\ \beta_t = \frac{2-\sigma_t}{\sigma_t}\frac{2\gamma}{\gamma+1}\frac{1}{P_r}, \\ \beta_n &= \frac{2-\sigma_v}{\sigma_v}, Kn=\frac{\lambda}{b}, \xi=\frac{T_2-T_0}{T_1-T_0} \end{aligned}\right\} \quad (10)$$

The system of linear ordinary differential equations is solved analytically. The expressions for the temperature, velocity and the induced magnetic field are given by

$$U(y) = C_3 e^{M\sqrt{P_m(1+\lambda)}y} + C_4 e^{-M\sqrt{P_m(1+\lambda)}y} + \frac{(1+\lambda)}{PrS+M^2P_m}\left(C_2\sqrt{PrS}\cos\sqrt{PrS}\,y - C_1\sqrt{PrS}\sin\sqrt{PrS}\,y\right) \quad (11)$$

$$B(y) = C_5 y - MP_m\left[\frac{C_3}{M\sqrt{P_m(1+\lambda)}}e^{M\sqrt{P_m(1+\lambda)}y} - \frac{C_4}{M\sqrt{P_m(1+\lambda)}}e^{-M\sqrt{P_m(1+\lambda)}y} + \frac{1+\lambda}{PrS+M^2P_m}\left(C_2\sin\sqrt{PrS}\,y + C_1\cos\sqrt{PrS}\,y\right)\right] + C_6 \quad (12)$$

$$\theta(y) = C_1\cos\sqrt{PrS}\,y + C_2\sin\sqrt{PrS}\,y \quad (13)$$

The induced current density is given by

$$J = -\frac{dB}{dy} = -\left[C_5 - MP_m(C_3 e^{M\sqrt{P_m(1+\lambda)}y} + C_4 e^{-M\sqrt{P_m(1+\lambda)}y} + \frac{1+\lambda}{PrS+M^2P_m}\left(C_2\sqrt{PrS}\cos\sqrt{PrS}\,y - C_1\sqrt{PrS}\sin\sqrt{PrS}\,y\right)\right] \quad (14)$$

$$= -C_5 + MP_m\left[(C_3 e^{M\sqrt{P_m(1+\lambda)}y} + C_4 e^{-M\sqrt{P_m(1+\lambda)}y} + \frac{1+\lambda}{PrS+M^2P_m}\left(C_2\sqrt{PrS}\cos\sqrt{PrS}\,y - C_1\sqrt{PrS}\sin\sqrt{PrS}\,y\right)\right] \quad (15)$$

where $A_1, A_2, A_3, A_4, A_5, A_6, A_7, A_8, A_9, A_{10}$, C_1, C_2, C_3, C_4, C_5, are all constants given in the Appendix.

Two important parameters for buoyancy-induced micro-flow are the volume flow rate (Q_m) and skin friction (τ). The dimensionless volume flow rate is

$$Q_m = \int_0^1 U(y)\,dy \quad (16)$$

$$= \left(\frac{C_3}{M\sqrt{P_m}}e^{M\sqrt{P_m(1+\lambda)}} - \frac{C_4}{M\sqrt{P_m}}e^{-M\sqrt{P_m(1+\lambda)}}\right.$$

International Journal of Advances in Engineering and Management (IJAEM)
Volume 4, Issue 5 May 2022, pp: 1190-1205 www.ijaem.net ISSN: 2395-5252

$$+\frac{1+\lambda}{PrS+M^2P_m}\left[C_2\sin\sqrt{PrS}+C_1\cos\sqrt{PrS}\right]\Bigg)$$
$$-\left(\frac{C_3}{M\sqrt{P_m}}-\frac{C_4}{M\sqrt{P_m}}+\frac{C_1(1+\lambda)}{PrS+M^2P_m}\right)$$
$$=\frac{C_3}{M\sqrt{P_m}}\left(e^{M\sqrt{P_m(1+\lambda)}}-1\right)-\frac{C_4}{M\sqrt{P_m}}\left(e^{-M\sqrt{P_m(1+\lambda)}}-1\right)$$
$$+\frac{C_1(1+\lambda)}{PrS+M^2P_m}\left(\cos\sqrt{PrS}-1\right)+\frac{C_2(1+\lambda)}{PrS+M^2P_m}\sin\sqrt{PrS}$$

(17)

Using expression (11), the skin-friction on both micro-channel plates in non-dimensional form are given by

$$\tau_0=\left.\frac{dU}{dy}\right|_{y=0}=C_3M\sqrt{P_m(1+\lambda)}-C_4M\sqrt{P_m(1+\lambda)}-\frac{C_1PrS(1+\lambda)}{PrS+M^2P_m} \quad (18)$$

$$\tau_1=\left.\frac{dU}{dy}\right|_{y=1}=C_3M\sqrt{P_m(1+\lambda)}\,e^{M\sqrt{P_m}}-C_4M\sqrt{P_m(1+\lambda)}\;e^{-M\sqrt{P_m(1+\lambda)}}$$
$$+\frac{1+\lambda}{PrS+M^2P_m}\left(-C_2PrS\sin\sqrt{PrS}-C_1PrS\cos\sqrt{PrS}\right) \quad (19)$$

III. RESULTS AND DISCUSSION

The governing equations have been solved analytically and numerically. The effects of pertinent parameters such as rarefaction parameter, fluid wall interaction parameters, induced magnetic field and wall ambient temperature difference have been depicted through graph. The numerical values assigned to the parameters are within reasonable ranges $0\le\beta_nKn\le0.1$ and $0\le Pn\le10$. The product β_nKn is a measure of the departure from the continuum regime whereas Pn is related to fluid wall interaction. The important aspect of discussion are (i) Variation of induced magnetic field, (ii) Induced current density.

Fig.2(a) shows the velocity distribution in a micro channel showing the effect of heat source / sink and β_nKn, aparameter measuring the departure from the continuum regime and the rarefaction parameter. The profiles are symmetrical about the middle of the channel and the velocity increases as the volumetric heat source parameter increases. The reverse effect is observed in case of sink. The reason for increase in velocity is straight forward as an additional heat source enhances the thermal energy giving rise to higher momentum transfer consequently, the velocity increases. It is further seen that an increase in rarefaction parameter β_nKn also enhances the velocity.

The velocity distribution is pertaining to the fixed values of $Pn=1.66, M=5, Pm=0.5$, $Pr=0.71, \xi=1, \lambda=0.$ The elastic parameter $\lambda=0$ and $Pr=0.71$ indicates the distribution is related to only viscous fluid.When $\xi=1$, both the plates are at equal temperature.

Fig. 2(b) brings out the effect of elastico-viscous parameter λ (the ratio of relaxation time of stress to retardation time of strain rate) for λ =0,1.1, 1.2. This shows that an increase in λ, and β_nKn both increase the velocity significantly throughout the channel maintaining the symmetricity about the middle layers. This indicates that for higher values of λ, i.e. for more relaxation time, more strain energy is being stored when the fluid is subject to applied stress. This is absolutely due to physical properties of the fluid in motion.

Fig 3(a) shows the effect of induced magnetic field along the width of channel in response to variation of heat source and rarefaction parameter. The

International Journal of Advances in Engineering and Management (IJAEM)
Volume 4, Issue 5 May 2022, pp: 1190-1205 www.ijaem.net ISSN: 2395-5252

striking feature of the variation is that the flauctuative velocity distribution remains invariant at the middle of the channel irrespective of the changes in heat source / sink strength and rarefaction parameters. This shows the compatibility of the induced magnetic field at the middle layer without being affected by the variations of S and $\beta_n Kn$. Further, it is seen that both S and $\beta_n Kn$ enhance the induced magnetic field in the lower half and the reverse effect is observed in the upper half.

Fig.3(b) shows that the induced magnetic field distribution. The fluctuative nature of the distribution remains same as that of 3(a) only escalation in magnitude occurs due to elasticity vis-a-vis energy stored under the impact of applied stress. The increase in velocity is nearly 2.5 times more than that of viscous flow $(\lambda = 0)$ Fig. 2(b).

The figures 2(a)(b) and 3(a)(b) show the novelty of the findings of the present study in comparison with figs. 2(c) and 3(c) which depict the case of without elasticity and without heat source. Figs. 2(a) and 3(a) represent the case of presence of heat source but absence of elasticity and figs 2(b), 3(b) show the presence of both heat source and elasticity, figs 2(c), 3(c) show the absence of both heat source and elasticity.

The comparison of above figures exhibit the novelity of the present study that thermal energy associated with material property i.e., elastic property maintains the symmetricity in both velocity and induced magnetic field distributions which is desirable and in some cases essential evidenced by fig 2(c) and 3(c) where the profiles exhibit three layers character with lack of symmetricity.

Following discussion pertains to purely viscous fluid. From figs 4 and 5 following observations are made. The fig.4 exhibits the case of viscous (λ =0) and $\xi = 1$ i.e. two plates are at equal temperature. In the absence of heat source $(S = 0)$ the temperature distribution is linear which is evident from $\frac{d^2T}{dy^2} = 0$. For $S \neq 0$, the temperature distribution is symmetric about the middle of the channel with an increase in strength of heat source. In case of sink $(S < 0)$, the distribution is a mirror reflection about the profile $S = 0$.

Fig.5 exhibits the velocity distribution in case of $\xi = 0$, i.e. $(T_2 = T_0$ and $T_1 \neq T_0)$ which implies upper plate is equal to ambient temperature. On careful observation and comparison with fig.2(a) ($\xi = 1$, equal plate temperature), it is seen that the profiles are asymmetric which is consequence of unequal plate temperature $(\xi = 0)$.

Fig.6 in comparison with fig. 6.4 exhibit a remarkable temperature distribution featuring the importance of bounding surface temperature $\xi = 0$, i.e. one plate is at ambient temperature and other plate is at arbitrarily assigned temperature. The variation is almost linear with three layered character with three invariant points depending upon (i) presence of sink, (ii) without source/sink and (iii) presence of source $(S = -1, 0, 1)$. Thus, it is concluded that heat energy flowing from bounding surface causes energy-level difference with ambient state resulted in almost linear temperature distribution with higher level of invariant layers commensurate with the strength of heat source and rarefaction parameter. This is a noteworthy phenomenon to record for any design requirement of heat exchanger.

Fig. 7 exhibits the velocity distribution for $\xi = -1$ which implies temperature of one plate is equal to negative of the other $(T_2 = -T_1)$ which is also evidenced by the computational result. This distribution is symmetric about the middle layer of the channel $y = 0.5$ and about y-axis. Consequently, the reverse effects are observed in respect of source and rarefaction parameter. This distribution also contributes significantly to the design of heat exchanger. To sum up, heating one plate of the channel (positive temperature) and cooling of the other plate at the same rate (negative temperature) greatly affects the temperature distributions.

Fig. 8 also presents a striking distribution of induced magnetic field for $\xi = -1$, i.e. positive and negative temperature of bounding surfaces. The change is evidenced by comparing fig.8 with fig.3(a). The oscillation of induced magnetic field is completely eradicated resulting in a smooth parabolic variation with maximum at the middle of the channel. This distribution retains the property of heat source and rarefaction parameters presented in earlier graphs. Thus, it is inferred that temperature of bounding surface greatly affects the velocity boundary layer and induced magnetic field substantially.

Examining the fig. 9, it is observed that reverse heating process of two bounding surfaces has a linearising effect on temperature distribution which is clear from figs.4 and 9. This invariance

International Journal of Advances in Engineering and Management (IJAEM)
Volume 4, Issue 5 May 2022, pp: 1190-1205 www.ijaem.net ISSN: 2395-5252

and symmetricity properties remain same as that of velocity boundary layer (fig.7).

It is interesting to record that reverse heating (positive temperature and negative temperature) condition at the plates sets a fluctuation in velocity field whereas a monotonic increase in temperature distribution is marked within the channel. The results may serves as a guideline for designing of heat transfer devices.

Table 1 presents the skin frictions at the lower plate τ_0, upper plate τ_1 and Nusselt number (Nu). The skin friction at the lower plate τ_0 remains positive for $\xi = 0$ and $\xi = 1.0$. But when $\xi = -1$ (i.e. the plates are subjected to positive temperature at one plate and negative at the other), it becomes negative. This indicates flow stability in case of plates are of opposite temperature.

Further, it is seen that presence of sink reduces the skin friction at both the plates for $\xi = 0$ and $\xi = -1$ but presence of source increases the skin friction for $\xi = 1.$ Reviewing the rate of heat transfer at the plate it is seen that an increase in rarefaction parameter reduces the Nusselt number.

To conclude, the reverse heating at the plates and application of transverse magnetic field and fluid wall interaction parameter reduce the shearing stress at the plates but the presence of heat source acts adversely. Moreover, rate of heat transfer at the plates depletes due to the presence of sink and gets enhanced due to source.

IV. CONCLUSION

- The rarefaction parameter $\beta_n Kn$, the heat source and elasticity accelerate the flow of Jeffrey fluid under investigation.
- The heat source combined with material property i.e. elasticity maintains symmetricity in velocity as well as induced magnetic field.
- The heat energy flowing from bounding surface causes energy level difference resulted in almost linear temperature distribution with higher level of invariant layers commensurate with the strength of heat source and rarefaction parameter.
- Reverse heating (positive temperature at one plate and negative temperature at the other) sets a fluctuation in velocity field. The reverse heating of the plates resulted in change of signs in skin friction at the plates. Increase in rarefaction parameter enhances the rate of heat transfer at the plates.

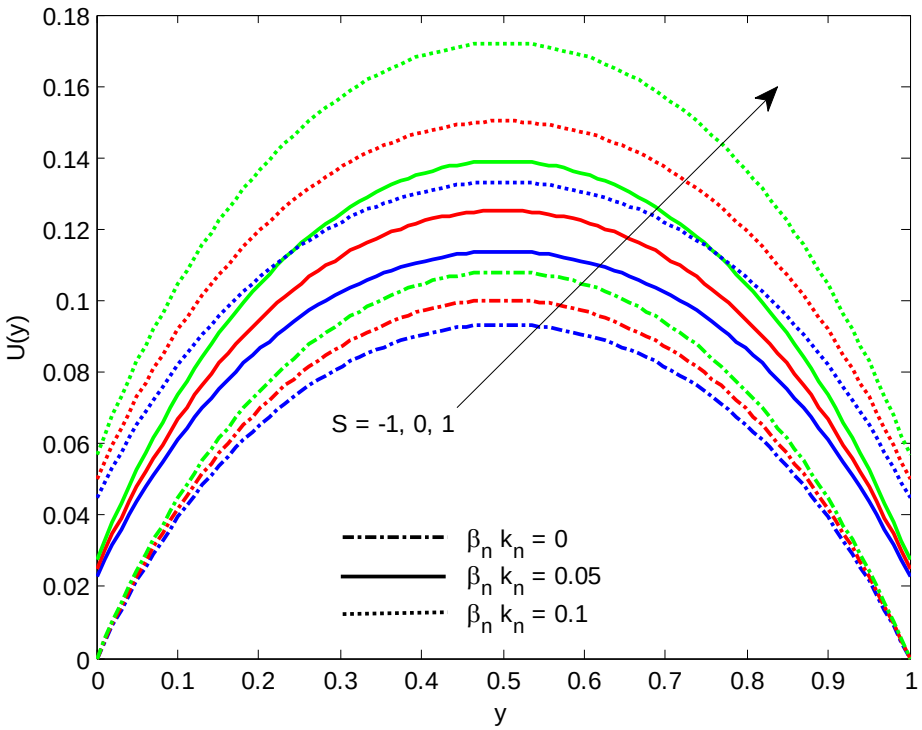

Fig.2(a):Velocity Profile for Pn =1.667, M=5, Pm = 0.5, Pr = 0.71, ξ_1 = 1, λ_1 = 0

International Journal of Advances in Engineering and Management (IJAEM)
Volume 4, Issue 5 May 2022, pp: 1190-1205 www.ijaem.net ISSN: 2395-5252

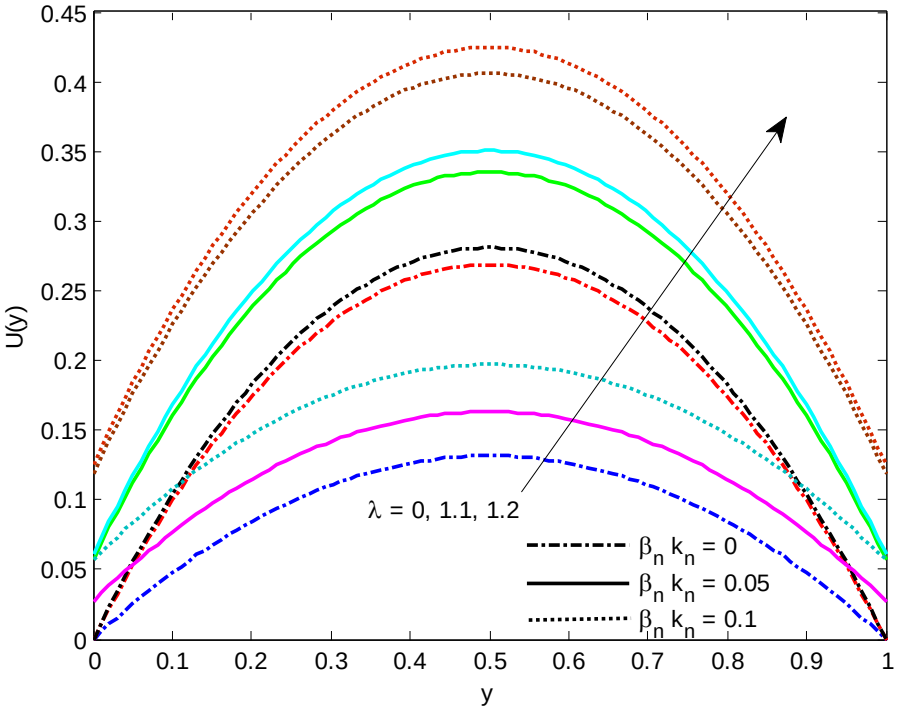

Fig.2(b) :Velocity Profile for Pn =1.667, M=5, Pm = 0.5, Pr = 0.71, ξ_1 = 1

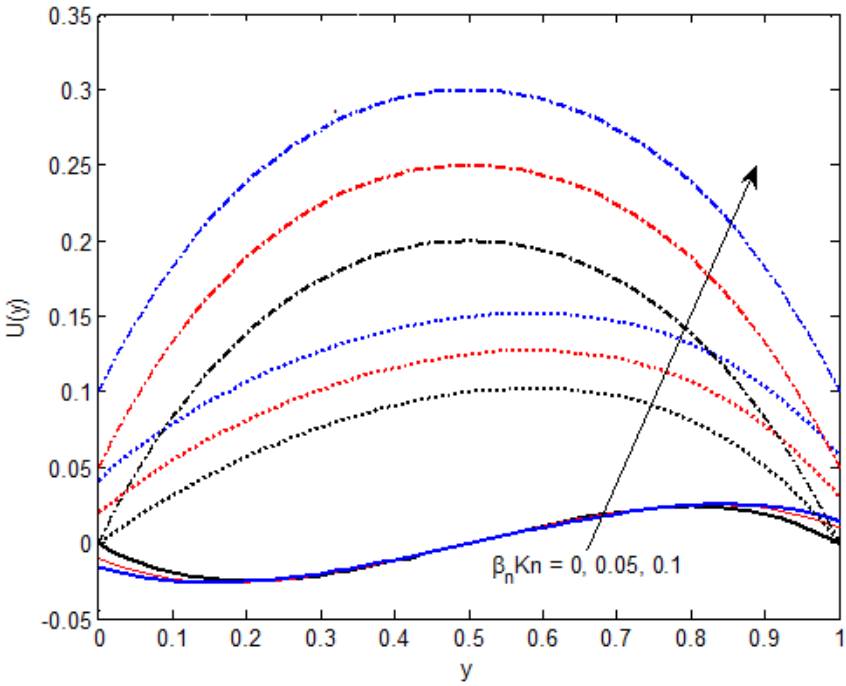

Fig.2(c): Velocity Profile for Pn =1.667, M=5, Pm = 0.5, Pr = 0.71, S=0, λ=0

International Journal of Advances in Engineering and Management (IJAEM)
Volume 4, Issue 5 May 2022, pp: 1190-1205 www.ijaem.net ISSN: 2395-5252

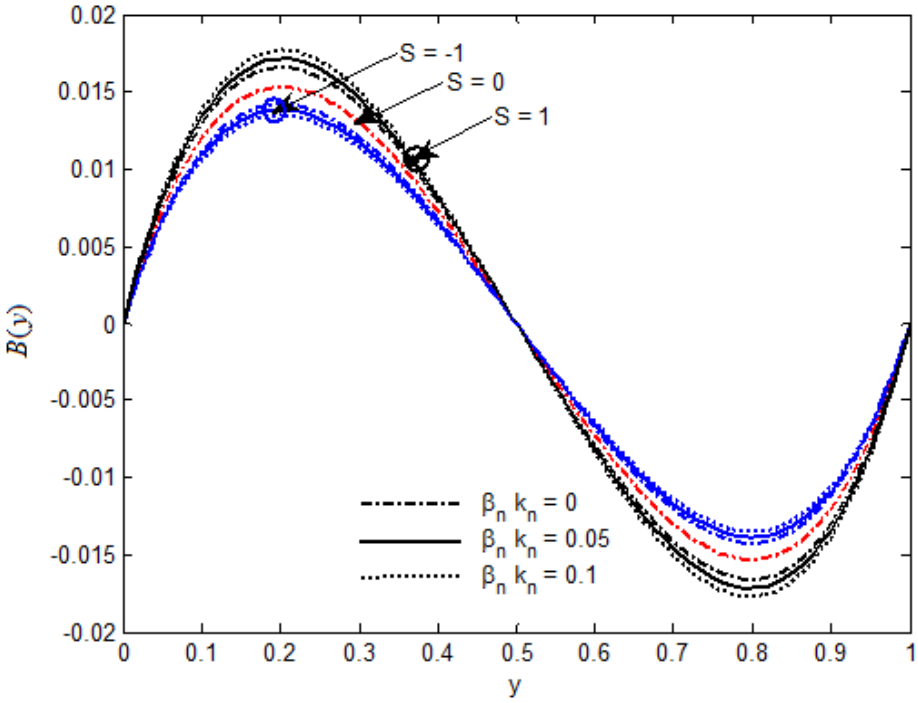

Fig.3(a): Induced magnetic field Profile for Pn =1.667, M=5, Pm = 0.5, Pr = 0.71, ξ_1 =1

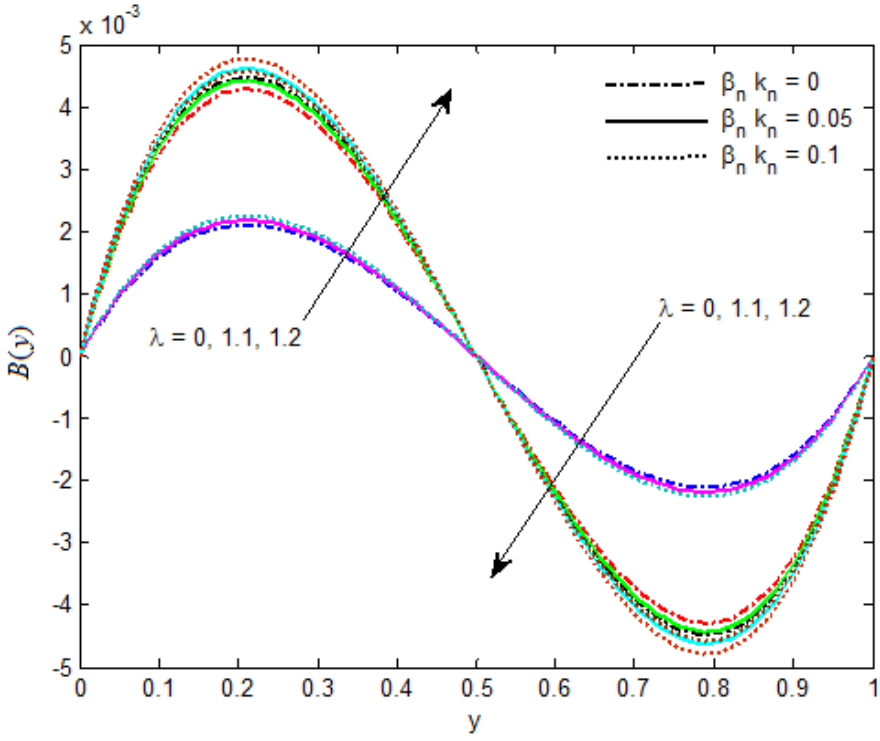

1

Fig.3(b) :Induced magnetic field Profile for Pn =1.667, M=5,Pm = 0.5,Pr = 0.71, ξ_1 = 1

International Journal of Advances in Engineering and Management (IJAEM)
Volume 4, Issue 5 May 2022, pp: 1190-1205 www.ijaem.net ISSN: 2395-5252

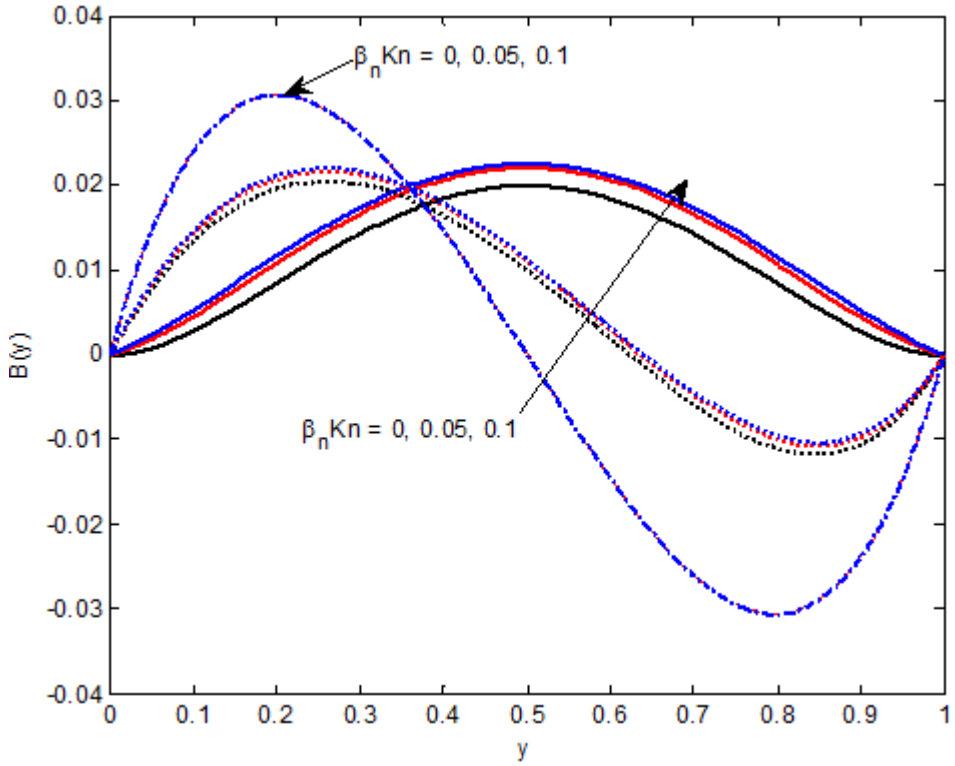

Fig.3(c): Induced magnetic field Profile for Pn =1.667, M=5,Pm = 0.5, S=0, λ=0

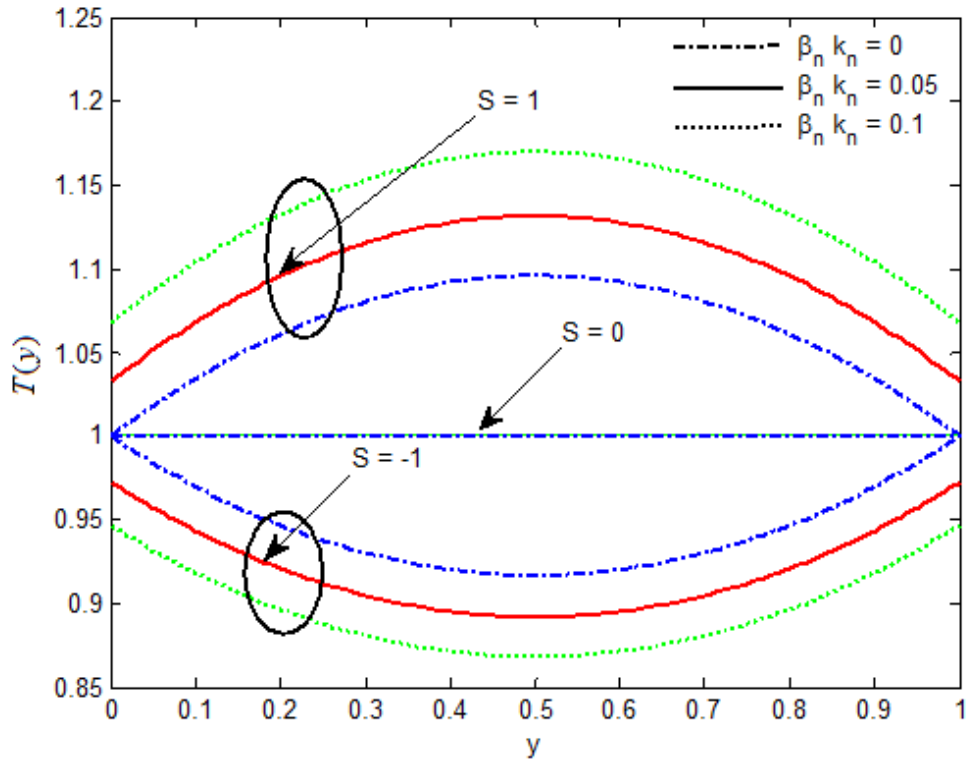

Fig.4: Temperature Profile for Pn =1.667, M=5, Pm = 0.5,Pr =0.71, ξ = 1

International Journal of Advances in Engineering and Management (IJAEM)
Volume 4, Issue 5 May 2022, pp: 1190-1205 www.ijaem.net ISSN: 2395-5252

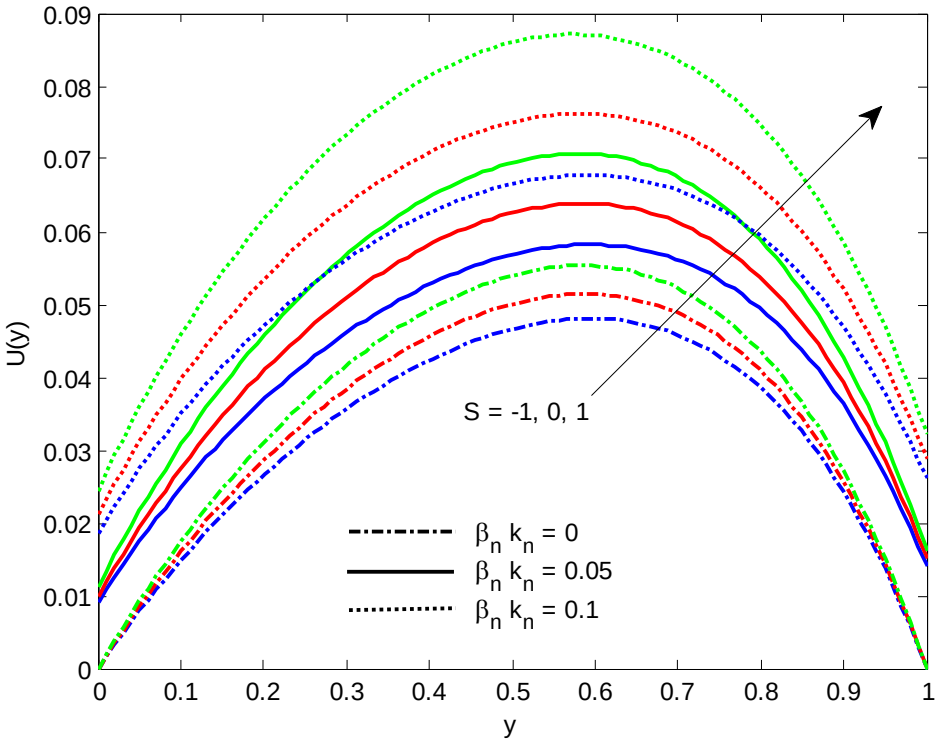

Fig. 5 : Velocity Profile for Pn =1.667, M=5, Pm = 0.5, Pr = 0.71, ξ = 0

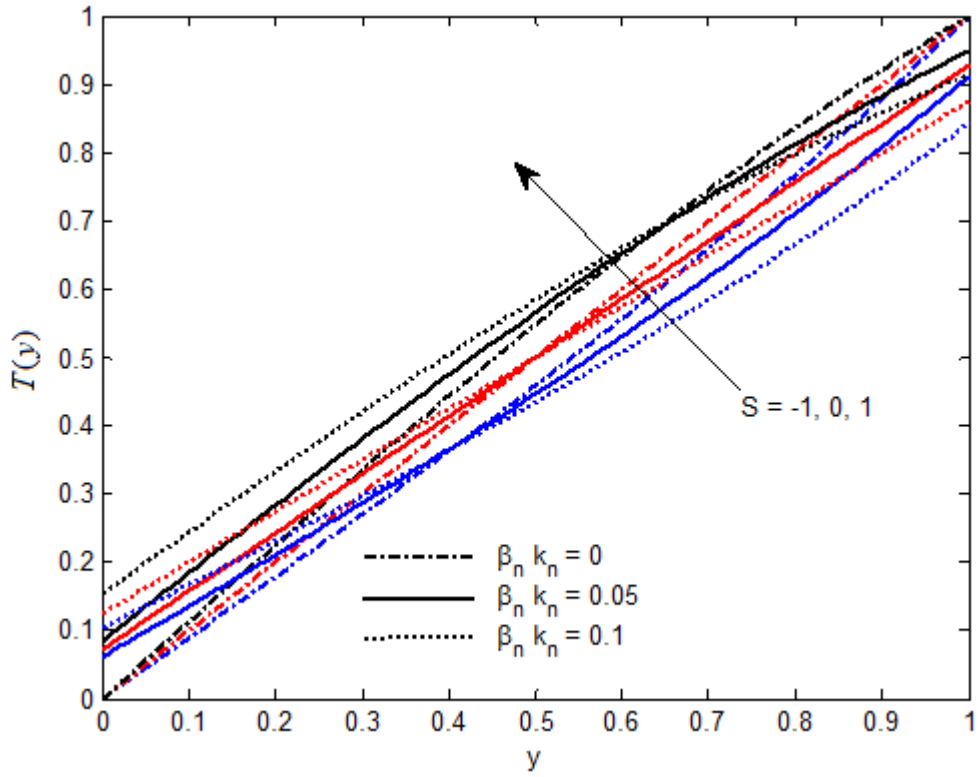

Fig.6: Temperature Profile for Pn =1.667, M=5, Pm = 0.5,Pr =0.71, ξ = 0

International Journal of Advances in Engineering and Management (IJAEM)
Volume 4, Issue 5 May 2022, pp: 1190-1205 www.ijaem.net ISSN: 2395-5252

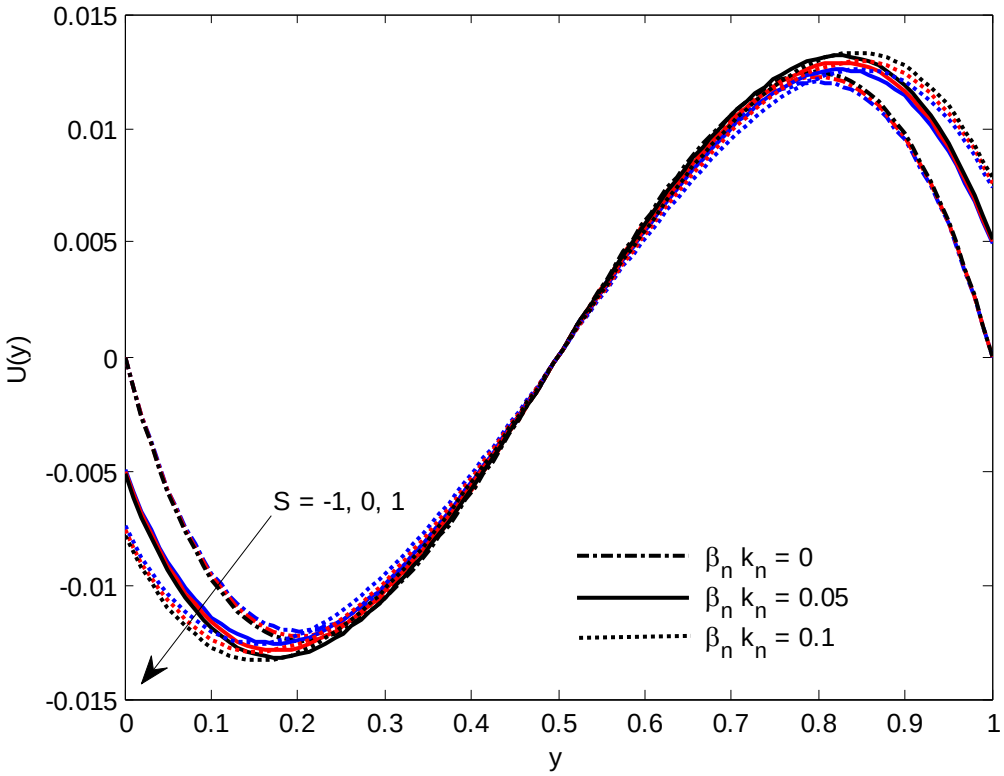

Fig.7: Velocity Profile for Pn =1.667, M=5, Pm = 0.5, Pr = 0.71, ξ =-1

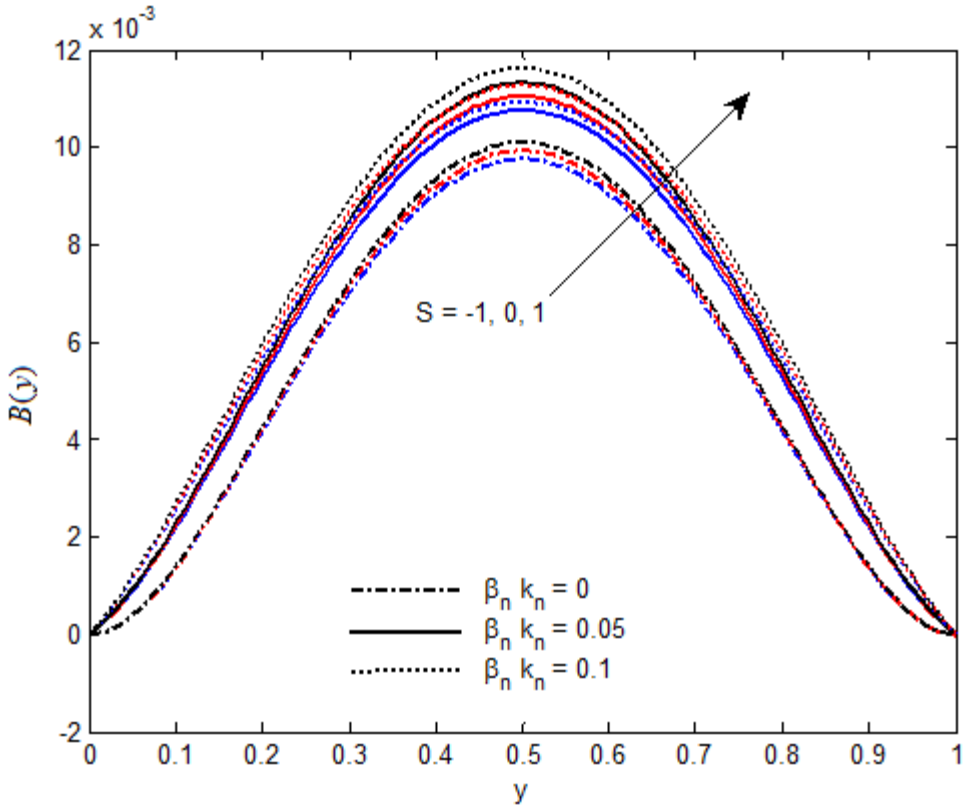

Fig.8: Induced magnetic field Profile for Pn =1.667,M=5,Pm = 0.5,Pr = 0.71, ξ = -1

International Journal of Advances in Engineering and Management (IJAEM)
Volume 4, Issue 5 May 2022, pp: 1190-1205 www.ijaem.net ISSN: 2395-5252

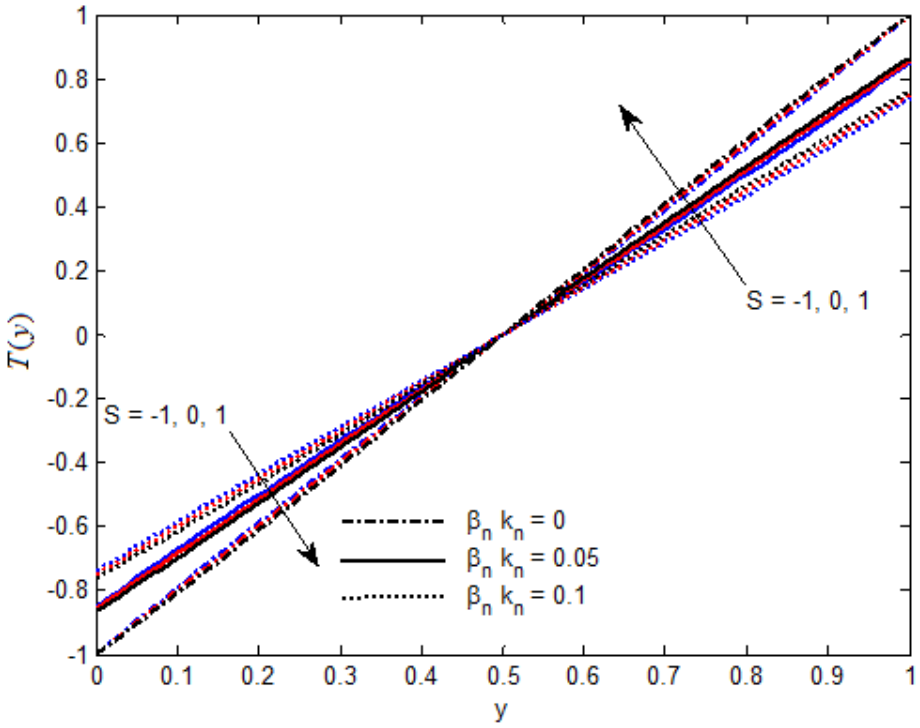

Fig. 9: Temperature Profile for Pn =1.667,M=5,Pm = 0.5,Pr = 0.71, ξ =-1

Table-1 : Skin friction coefficient and Nusselt number Pn=1.667,Pr =0.71

$\beta_n Kn$	M	Pm	ξ	S	τ_0	Jha et al.[12]	τ_1	Jha et al.[12]	Nu	Jha et al.[12]
0	5	0.5	-1	0	-0.13982	-0.13979	-0.13982	-0.13979	-1.99999	-1.99999
0.05	5	0.5	-1	0	-0.10093	-0.10092	-0.10093	-0.10092	-1.71423	-1.71397
0.05	3	0.5	-1	0	-0.11734	-0.11712	-0.11734	-0.11712	-1.71423	-1.71397
0.05	5	10	-1	0	-0.02645	-0.02638	-0.02645	-0.02645	-1.71423	-1.71397
0.05	5	0.5	0	0	0.186965	0.186946	-0.31303	-0.31297	-0.85712	-0.85632
0.05	5	0.5	1	0	0.499999	0.499873	-0.5	-0.49999	-0.20314	-0.20289
0.05	5	0.5	-1	-1	-0.12358	-0.12347	-0.12358	-0.12347	-1.79944	-1.79901
0.05	5	0.5	0	-1	0.167974	0.167875	-0.29156	-0.29123	-0.73659	-0.73612
0.05	5	0.5	1	-1	0.459529	0.459432	-0.45953	-0.45879	0.326266	0.326203
0.05	5	0.5	-1	1	-0.12867	-0.12852	-0.12867	-0.12852	-1.62549	-1.62498
0.05	5	0.5	0	1	0.210227	0.210194	-0.3389	-0.33734	-1.00769	-1.00702
0.05	5	0.5	1	1	0.549128	0.549028	-0.54913	-0.5489	-0.38988	-0.38912

BIBLIOGRAPHY

[1] S. Yu, T.A. Ameel (2001).Slip-flow heat transfer in rectangular microchannels,Int. J. Heat mass transfer, **44**, 4225-4234.

[2] J.Q. Liu, Y.C. Tai, C.M. Ho (1995). MEMS for pressure distribution studies of gaseous flow in microchannels, Proc. IEEE Micro-electromech.Syst., 209-215.

[3] E.B. Arkilic, K.S. Breuer, M.A. Schimdth (1994). Gaseous flow in microchannels, Application of Micro-fabrication to fluid Mechanics, ASME FWD, **197**, 57-66.

[4] Y.P. Shih, C.C. Huang, S.Y. Tsay (1995). Extended Leveque solution for laminar heat transfer to power-law fluids in pipes with wall slip, Int. J. Heat Mass Transfer, 38, 403-408.

[5] R. F. Barron, X.M. Wang, R.O. Warrington, T.A. Ameel (1996). Evaluation of the eigenvalues for the Graetz problem in slip-flow, Int. Commun.Heat Transfer, **23**, 563-574.

[6] R. F. Barron, X.M. Wang, T.A. Ameel and R.O. Warrington (1997). The Graetz problem extended to slip-flow, Int. J. Heat Mass Transfer, **40**, 1817-1823.

[7] X.M. Wang (1996). Evaluation of the eigenvalues of the Graetz problem in slip-flow, M.S. Thesis, Louisiana Tech University, Ruston, Louisiana.

[8] L. Biswas, S.K. Som and S. Chakraborty (2007). Effects of entrance region transport processes on free convection slip flow in vertical microchannels with isothermally heated walls. Int. J. Heat Mass Transfer, 50, 1248-54.

[9] J.L. Manganaro and O.T. Hanna (1970). Simultaneous energy and mass transfer in the laminar boundary layer with large mass transfer rates toward the surface AIChE J.,16 (2), 204.

[10] D.A. Saville and S.W. Churchill (1967).Laminar free convection in boundary layers near horizontal cylinders and vertical axisymmetric bodies, J. Fluid Mech, **29**, 391.

[11] D.A. Saville and S.W. Churchill (1970).Simultaneous heat and mass transfer in free convection boundary layers,AIChE J., **16,** 268.

[12] B.K. Jha, BabatundeAina and A.T. Ajiya (2015).MHD natural convection flow in a vertical parallel plate microchannel, Ain Shams Engg. J., **6,** 289-295.

[13] B.K. Jha, BabatundeAina and Isa Sani (2015). Fully developed MHD natural convection flow in a vertical annular microchannel: An exact solution, Journal of King Saud University- Science, **27**, 253-259.

[14] R.K. Singh, A.K. Singh, N.C. Sachetiand P. Chandran (2010). On hydromagnetic free convection in the presence of induced magnetic field, Heat Mass Transfer, 46, 523-529.

[15] S.K.Ghosh, O.A. Beg and J. Zueco (2010). Hydromagnetic free convection flow with inducedmagnetic field effects, Meccanica, 14, 175-185.

[16] Sarveshanand, A.K. Singh Magnetohydrodynamic free convection between vertical parallel porous plate in the presence of induced magnetic field, SpringerPlus, DOI 10.1186/s40064-015-1097-1.

[17] C.K.Chen and H.C. Wang (2005). Natural Convection in a Vertical Microchannel, J. Heat Transfer, 127, 1053-1056.

[18] E.R.G. Eckert and R.M. Drake, Jr. (1972).Analysis of Heat and Mass Transfer, Mcgraw-Hill, New York, chap. 11.

[19] W.M. Rohsenow and J.P. Hartnett (1973).Handbook of Heat Transfer, Mcgraw-Hill, New York, chap. 9.

[20] R. Goniak and G. Duffa (1995).Corrective Term in Wall Slip Equations for Knudsen layer, J. Thermophys. Heat Transfer, **9,** 383-384.

International Journal of Advances in Engineering and Management (IJAEM)
Volume 4, Issue 5 May 2022, pp: 1190-1205 www.ijaem.net ISSN: 2395-5252

Nomenclature

b the gap between the plates
u' velocity of the fluid in the x' -direction
g gravitational acceleration
C_p specific heat
P_m magneticPrandtl number
T' dimensional temperature of the fluid
T dimensionless temperature of the fluid
U dimensionless velocity
M Magneticparameter
Kn Knudsen number
G_r thermalGrashof number
D_m mass diffusivity
$\vec{B}$ Magnetic field vector
B_0' Uniform magnetic field strength
$B_{x'}'$ induced magnetic field
B_0 constant magnetic flux density
B dimensionless induced magnetic fi
J induced current density
Pr Prandtl number
Pn fluid-wall (temperature dependent)interaction parameter
Q_m volume flow rate
Q_0 volumetric heat source
Nu Nusselt number
T_1 temperature of the hotter plate
T_2 temperature of the cooler plate
T_0 free stream temperature

Greek symbols

α thermal diffusivity
β volumetric coefficient of thermal expansion
β' volumetric coefficient of expansion with concentration
ν kinematic viscosity
ρ density
μ_e magnetic permeability
λ The ratio of relaxation of stress to retardation time of strain
λ_1 molecular mean free path
γ ratio of specific heats
μ dynamic viscosity
τ skin friction
σ_v tangential momentum coefficient
σ_t thermal accommodation coefficient

International Journal of Advances in Engineering and Management (IJAEM)
Volume 4, Issue 5 May 2022, pp: 1190-1205 www.ijaem.net ISSN: 2395-5252

σ electrical conductivity of the fluid

β_n, β_t dimensionless variables

ξ wall-ambient temperature ratio

Appendix

$$A_1 = \beta_v Kn\, In$$

$$C_1 = \xi + A_1 C_2 \sqrt{Pr\, S}$$

$$C_2 = \frac{1-\xi(\cos\sqrt{P_r S} - A_1\sqrt{P_r S}\sin\sqrt{P_r S})}{2A_1\sqrt{P_r S}\cos\sqrt{P_r S} + (1-A_1^2 P_r S)\sin\sqrt{P_r S}}$$

$$A_2 = \beta_v Kn$$

$$A_3 = 1 - A_2 M\sqrt{P_m(1+\lambda_2)}$$

$$A_4 = 1 + A_2 M\sqrt{P_m(1+\lambda_2)}$$

$$A_5 = -\frac{1+\lambda_2}{P_r S + M^2 P_m}\left(C_2\sqrt{P_r S} + C_1 P_r S A_2\right)$$

$$A_6 = e^{M\sqrt{P_m(1+\lambda_2)}} + A_2 M\sqrt{P_m(1+\lambda_2)}e^{M\sqrt{P_m(1+\lambda_2)}}$$

$$A_7 = e^{-M\sqrt{P_m(1+\lambda_2)}} - A_2 M\sqrt{P_m(1+\lambda_2)}e^{-M\sqrt{P_m(1+\lambda_2)}}$$

$$A_8 = \frac{(1+\lambda_2)}{P_r S + M^2 P_m}\left((C_1\sqrt{P_r S} + A_2 C_2 P_r S)\sin\sqrt{P_r S} - (C_2\sqrt{P_r S} - A_2 C_1 P_r S)\cos\sqrt{P_r S}\right)$$

$$A_9 = C_6$$

$$A_{10} = MP_m[\frac{C_3}{M\sqrt{P_m(1+\lambda_2)}}e^{m\sqrt{P_m(1+\lambda_2)}} - \frac{C_4}{M\sqrt{P_m(1+\lambda_2)}}e^{-M\sqrt{P_m(1+\lambda_2)}}$$

$$+\frac{1+\lambda_2}{P_r S + M^2 P_m}(C_2\sin\sqrt{P_r S} + C_1\cos\sqrt{P_r S})]$$

$$C_3 = \frac{A_5 A_7 - A_8 A_4}{A_3 A_7 - A_6 A_4}$$

$$C_4 = \frac{A_5 A_6 - A_8 A_3}{A_4 A_6 - A_7 A_3}$$

$$C_5 = A_{10} - A_9$$

$$C_6 = C_3\sqrt{\frac{P_m}{1+\lambda_2}} - C_4\sqrt{\frac{P_m}{1+\lambda_2}} + \frac{MP_m C_1(1+\lambda_2)}{P_r S + M^2 P_m}$$

• • •